The Observational Case for Jupiter
Being a Typical Massive Planet

Charles H. Lineweaver & Daniel Grether

University of New South Wales

charley@bat.phys.unsw.edu.au

ABSTRACT

We identify a subsample of the recently detected extrasolar planets that is minimally affected by the selection effects of the Doppler detection method. With a simple analysis we quantify trends in the surface density of this subsample in the period-$M \sin(i)$ plane. A modest extrapolation of these trends puts Jupiter in the most densely occupied region of this parameter space, thus indicating that Jupiter is a typical massive planet rather than an outlier. Our analysis suggests that Jupiter is more typical than indicated by previous analyses. For example, instead of M_{Jup} mass exoplanets being twice as common as $2\,M_{\mathrm{Jup}}$ exoplanets, we find they are three times as common.

1.   Exoplanets and the Standard Model of Planet Formation

The prevalence of infrared emission from accretion disks around young stars is consistent with the idea that such disks are ubiquitous. Their disappearance on a time scale of 50 to 100 million years suggests that the dust and gas accrete into planetesimals and eventually planets (Haisch *et al.* 2001). Such observations support the widely accepted idea that planet formation is a common by-product of star formation (e.g. Beckwith *et al.* 2000). In the standard model of planet formation, Earth-like planets accrete near the host star from rocky debris depleted of volatile elements, while giant gaseous planets accrete in the ice zones ($\gtrsim 4$ AU) around rocky cores (Lissauer 1995, Boss 1995). When the rocky cores in the ice zones reach a critical mass ($\sim 10\ m_{\mathrm{Earth}}$) runaway gaseous accretion (formation of jupiters) begins and continues until gaps form in the protoplanetary disk or the disk dissipates (Papaloizou & Terquem 1999, Habing *et al.* 1999), leaving one or more Jupiter-like planets at $\sim 4-10$ AU.

We cannot yet determine how generic the pattern described above is. However, formation of terrestrial planets is thought to be less problematic than the formation of Jupiter-like planets (Wetherill 1995). Gas in circumstellar disks around young stars is lost within a few million years and it is not obvious that the rocky cores necessary

to accrete the gas into a Jupiter can form on that time scale (Zuckerman *et al.* 1995). Thus, Jupiter-like planets may be rare. Planets may not form at all if erosion, rather than growth, occurs during collisions of planetesimals (Kortenkamp & Wetherill 2000). The present day asteroid belt may be an example of such non-growth. In addition, not all circumstellar disks produce an extant planetary system. Some fraction may spawn a transitory system only to be accreted by the central star along with the disk (Ward 1997). Also, observations of star-forming regions indicate that massive stars disrupt the protoplanetary disks around neighboring lower mass stars, aborting their efforts to produce planets (Henney & O'Dell 1999). Given these uncertainties, whether planetary systems like our Solar System are common around Sun-like stars and whether Jupiter-like planets are typical of such planetary systems, are important open questions.

The frequency of Jupiter-like planets may also have implications for the frequency of life in the Universe. A Jupiter-like planet shields inner planets from an otherwise much heavier bombardment by planetesimals, comets and asteroids during the first billion years after formation of the central star. Wetherill (1994) has estimated that Jupiter significantly reduced the frequency of sterilizing impacts on the early Earth during the important epoch ~ 4 billion years ago when life originated on Earth. The removal of comet Shoemaker-Levy by Jupiter in 1994, is a more recent example of Jupiter's protective role.

To date (November, 2001), 74 giant planets ($M\sin(i) < 13\ M_{\rm Jup}$) in close orbits ($< 4\ AU$) around 66 nearby stars have been detected by measuring the Doppler reflex of the host star (Marcy *et al.* 2001, Mayor *et al.* 2001). Seven stars are host to multiple planets (six doubles, one triple system). Approximately 5% of the Sun-like stars surveyed possess such giant planets (Marcy & Butler 2000). The large masses, small orbits, high eccentricities and high host metallicities of these 74 exoplanets was not anticipated by theories of planet formation that were largely based on the assumption that planetary systems are ubiquitous and our Solar System is typical (Lissauer 1995).

Naef *et al.* (2001) point out that none of the planetary companions detected so far resembles the giants of the Solar System. This observational fact however, is fully consistent with the idea that our Solar System is a typical planetary system. Fig. 1 shows explicitly that selection effects can easily explain the lack of detections of Jupiter-like planets. Exoplanets detected to date can not resemble the planets of our Solar System because the Doppler technique used to detect exoplanets has not been sensitive enough to detect Jupiter-like planets. If the Sun were a target star in one of the Doppler surveys, no planet would have been detected around it.

This situation is about to change. In the next few years Doppler planet searches will be making detections in the region of parameter space occupied by Jupiter. Thus
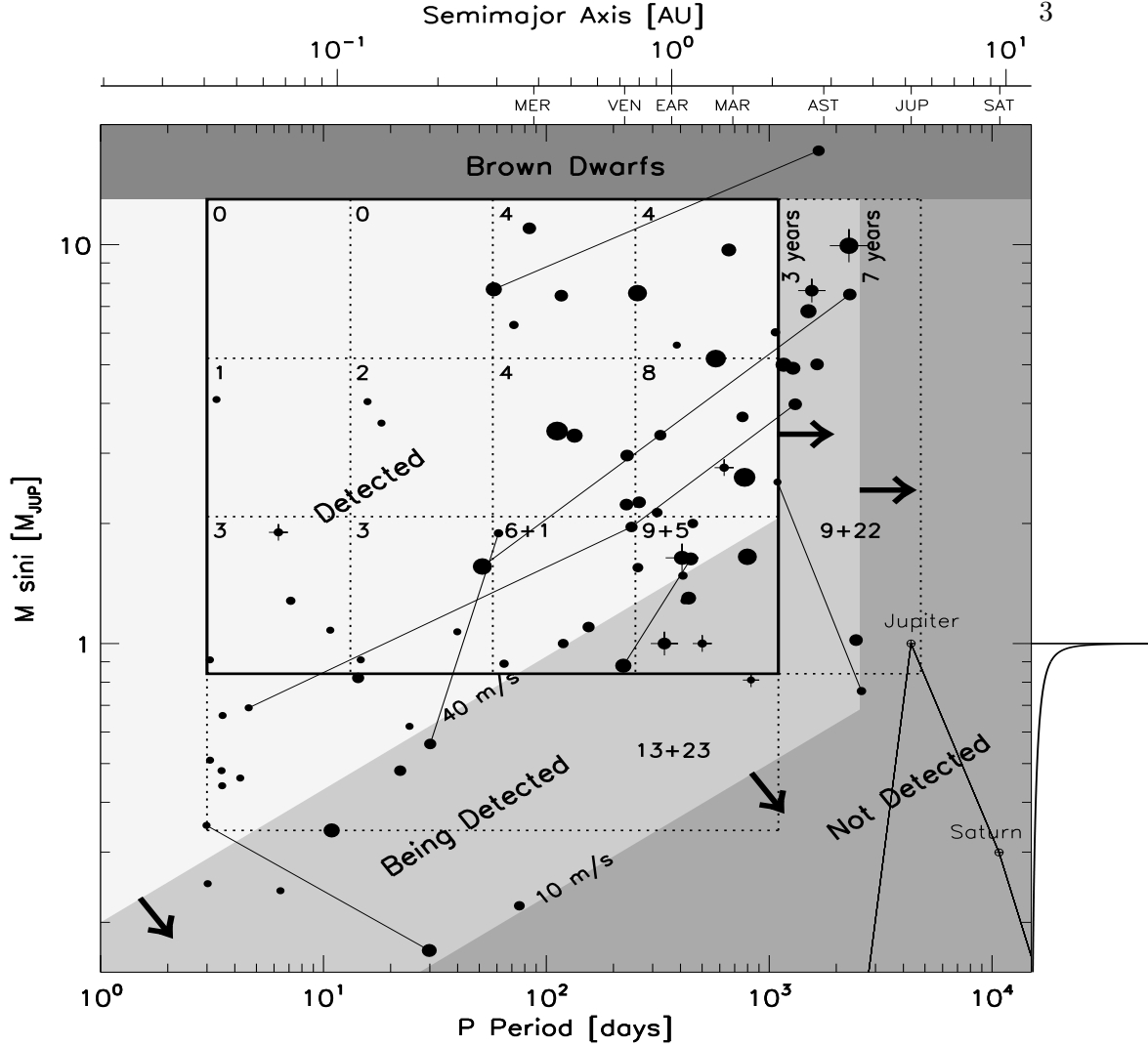
Fig. 1.— Mass as a function of period for the 74 exoplanets detected to date. Regions where planets are "Detected", "Being Detected" and "Not Detected" by the Doppler surveys are shaded differently and represent the observational selection effects of the Doppler reflex technique (see Section 2.1 for a description of these regions). The rectangle enclosing the grid of twelve boxes defines the subsample of 44 planets less biased by selection effects. The numbers in the upper left of each box gives the number of planets in that box. The increasing numbers from left to right and from top to bottom are easily identified trends. In Figs. 3 & 4 we quantify and extrapolate these trends into the lower mass bin and into the longer period bin which includes Jupiter. The "+1" and "+5" in the two boxes in the lower right refer to the undersampling corrections discussed in Section 2.2. The seven exoplanetary *systems* are connected by thin lines. Jupiter and Saturn are in the "Not Detected" region. The upper x axis shows the distances and periods of the planets of our Solar System. The brown dwarf region is defined by $M \sin(i)/M_{\mathrm{Jup}} > 13$. The point size of the exoplanets is proportional to the eccentricity of the planetary orbits.

it is timely to use the current data to estimate how densely occupied that parameter space will be. The detected exoplanets may well be the observable 5% tail of the main concentration of massive planets of which Jupiter is typical. The main goal of this paper is to correct or account for selection effects to the extent possible and then examine what the trends in the mass and period distributions indicate for the region of parameter space near Jupiter. Such an analysis is now possible because a statistically significant sample is starting to emerge from which we can determine meaningful distributions in mass, period as well as in eccentricity and metallicity. Our analysis helps answer the important question: How does our planetary system compare to other planetary systems?

In the next section we present our method for identifying a less biased subsample of exoplanets. In Section 2 we identify and extrapolate the trends in mass and period. In Section 3 we discuss our analysis and compare our results to previous work. In Section 4 we summarize our results.

2. Period-Mass Plane

2.1. Selection Effects

Doppler surveys are responsible for all 74 exoplanets plotted in Fig. 1. To detect an exoplanet, its host star must be Doppler-monitored regularly for a period P_{obs} greater than or comparable to the orbital period P of the planet. Thus, one selection effect on the detection of exoplanets is

$$P_{\mathrm{obs}} \gtrsim P. \tag{1}$$

The relationship between the observable line-of-sight velocity of the host star, $K = v_* \sin(i)$, the mass of the planet, M, the mass of the host star, M_*, the velocity of the planet, v_{p}, and the semi-major axis of the the planet's orbit, a, is obtained by combining $v_{\mathrm{p}} = (2\pi/P) \left[a/(1 - e^{1/2})\right]$ (where e is orbital eccentricity) with momentum conservation, $M_* K = M \sin(i)\, v_{\mathrm{p}}$, and Kepler's third law $M_* = \frac{a^3}{P^2}$ (in the limits that $M_* >> M$, and where M_*, a and P are measured in solar masses, AU and years respectively). Simultaneously solving these equations yields the induced line-of-sight velocity of the host star,

$$K = 2\pi \frac{M \sin(i)}{M_*^{2/3}} P^{-1/3} \left[\frac{1}{(1 - e^2)^{1/2}}\right]. \tag{2}$$

This equation is used to find $M \sin(i)$ as a function of the Doppler survey observables K, P and e, with M_* estimated from stellar spectra. To detect an exoplanet, the radial velocity K must be greater than the instrumental noise, K_{s}. Thus, the Doppler

technique is most sensitive to massive close-orbiting planets. Fig. 1 shows that we are now on the verge of being able to detect planetary systems like ours, i.e., Jupiter-mass planets at $\gtrsim 4$ AU from nearby host stars. The grey regions of Fig. 1 partition the parameter space and represent the selection effects of the Doppler surveys. We use these partitions to identify a less biased subsample of 44 exoplanets within the rectangular area enclosed by the thick solid line.

The largest observed P and the smallest observed K of the exoplanets in Fig. 1 are inserted into Equations 1 & 2 to empirically define the boundary between the "Being Detected" and the "Not Detected" regions in Fig. 1. To define the "Detected" region of parameter space in which virtually all planets should have been detected (thus defining a less biased subsample of exoplanets) we consider planets with $P < 3$ years with $K > 40$ m/s, that have been observed for more than 3 years with an instrumental noise $K_{\mathrm{s}} < 20$ m/s. The rectangle in Fig. 1 is the largest rectanglar area that approximately fits inside the "Detected" region. This method of cutting the data to remove biases is reminiscent of the astronomical practice of constructing a volume-limited sample from a magnitude-limited sample. The area within the rectangle subsumes the ranges $3 < P < 1000$ days and $0.84 < M\sin(i)/M_{\mathrm{Jup}} < 13$ and is subdivided into a minimum number of smaller areas (12 boxes) for histogram binning convenience (Figs. 3 & 4). Trends in $M\sin(i)$ and P identified within this subsample are less biased than trends based on the full sample of exoplanets.

If Jupiter is a typical giant planet, the region around Jupiter in the $P - M\sin(i)$ plane of Fig. 1 will be more densely occupied than other regions – the density of planets in the lower right will be larger than in the upper left. Although we are dealing with small number statistics, that trend is the main identifiable trend in Fig. 1; the number of exoplanets in the boxes increases from left to right and top to bottom. In the rest of the paper we quantify and extrapolate these trends into the lower mass bin and longer period bin enclosed by the dotted rectangles in Fig. 1.

2.2. Undersampling Corrections

Within the rectangle enclosed by the thick solid line in Fig. 1, two boxes in the lower right lie partially in the "Being Detected" region. Thus they are partially undersampled compared to the other boxes within the rectangle. We correct for this undersampling by making the simple assumption that the detection efficiency is linear in the "Being Detected" region. That is, we assume that the detection efficiency is 100% in the "Detected" region and 0% in the "Not Detected" region and decreases linearly inbetween. This linear correction produces the "+1" and "+5" corrections to the number of exoplanets observed in these two boxes and produces the dotted corrections to the histograms in Figs. 2, 3 and 4.
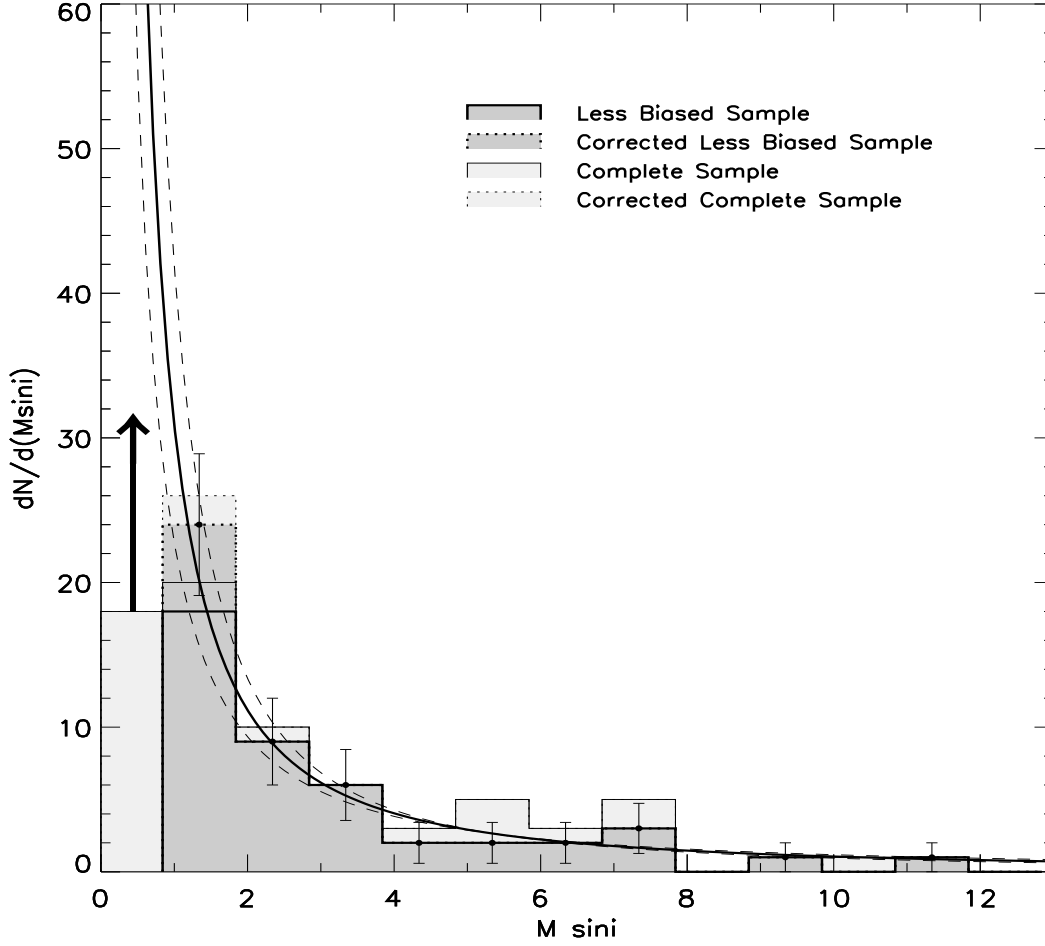
Fig. 2.— Mass histogram of the less-biased subsample (dark grey) of 44 exoplanets within the rectangle in Fig. 1 compared to the histogram of the complete sample of 74 exoplanets (light grey). The errors on the bin heights are Poissonian. The solid curve and the enclosing dashed curves are the best fit and 68% confidence levels from fitting the functional form $(dN/dM \sin i) \propto (M \sin i)^{\alpha}$ to the histogram of the corrected less-biased subsample ($50 = 44 + 6$ exoplanets). The extrapolation of this curve into the lower mass bin produces an estimate of the substantial incompleteness of this bin (arrow). The mass ranges of the bins are: $0.84, 1.84, 2.84...M \sin(i)/M_{\mathrm{Jup}}$. The lower limit of 0.84 was chosen to match the lower limit of the logarithmic binning in Fig. 1.
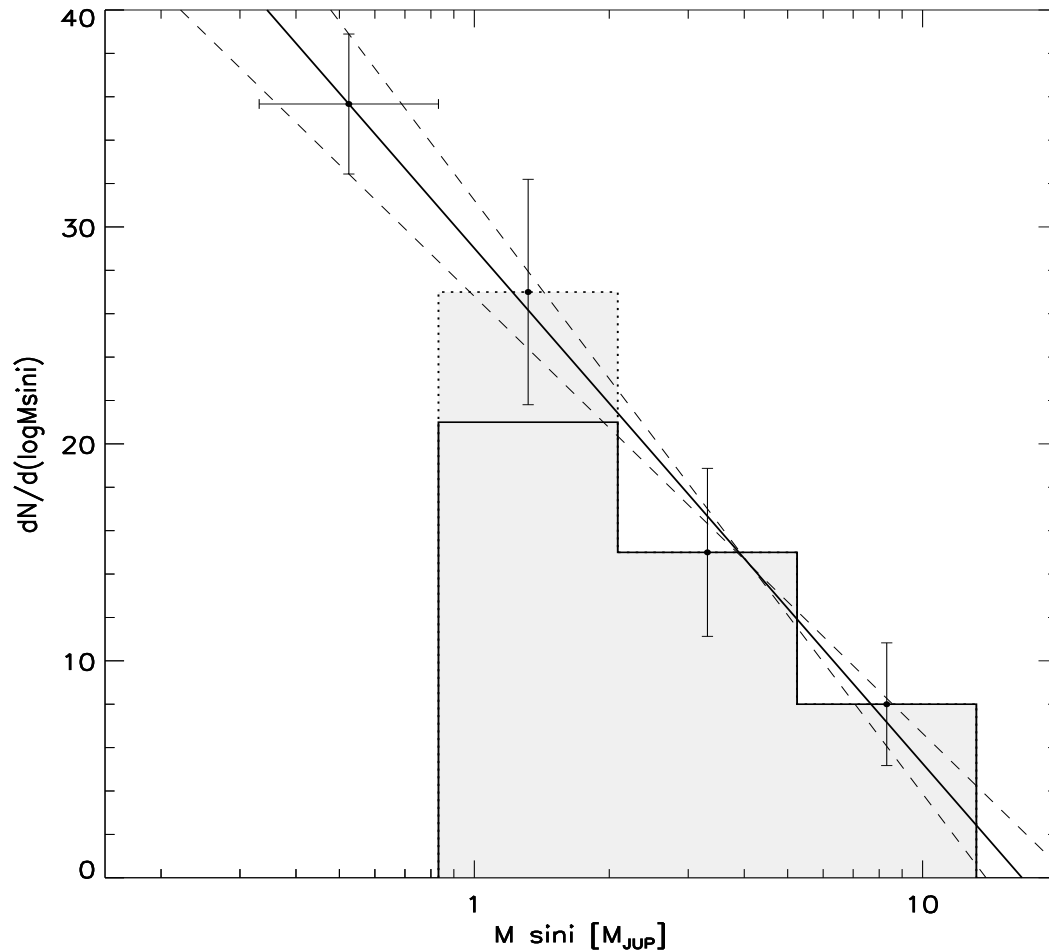
Fig. 3.— Histogram in $\log(M \sin i)$ of the 50 (= 44 + 6) exoplanets within the rectangular area enclosed by the thick solid line in Fig 1. The difference between the solid and dotted histograms in the lowest mass bin is the correction factor due to undersampling as described in Section 2.2. The line is the best fit to the functional form $dN/d(log(M \sin i)) = a \ log(M \sin i) + b$. The best fit slope is $a = -24 \pm 4$. The extrapolation of this trend into the adjacent lower mass bin ($0.34 < M \sin(i)/M_{\rm Jup} < 0.84$) indicates that at least $\sim 36 \pm 3$ exoplanets with periods in the range $3 - 1000$ days are being hosted by the target stars now being monitored. This is 23 more than the 13 that have been detected to date in this mass range.
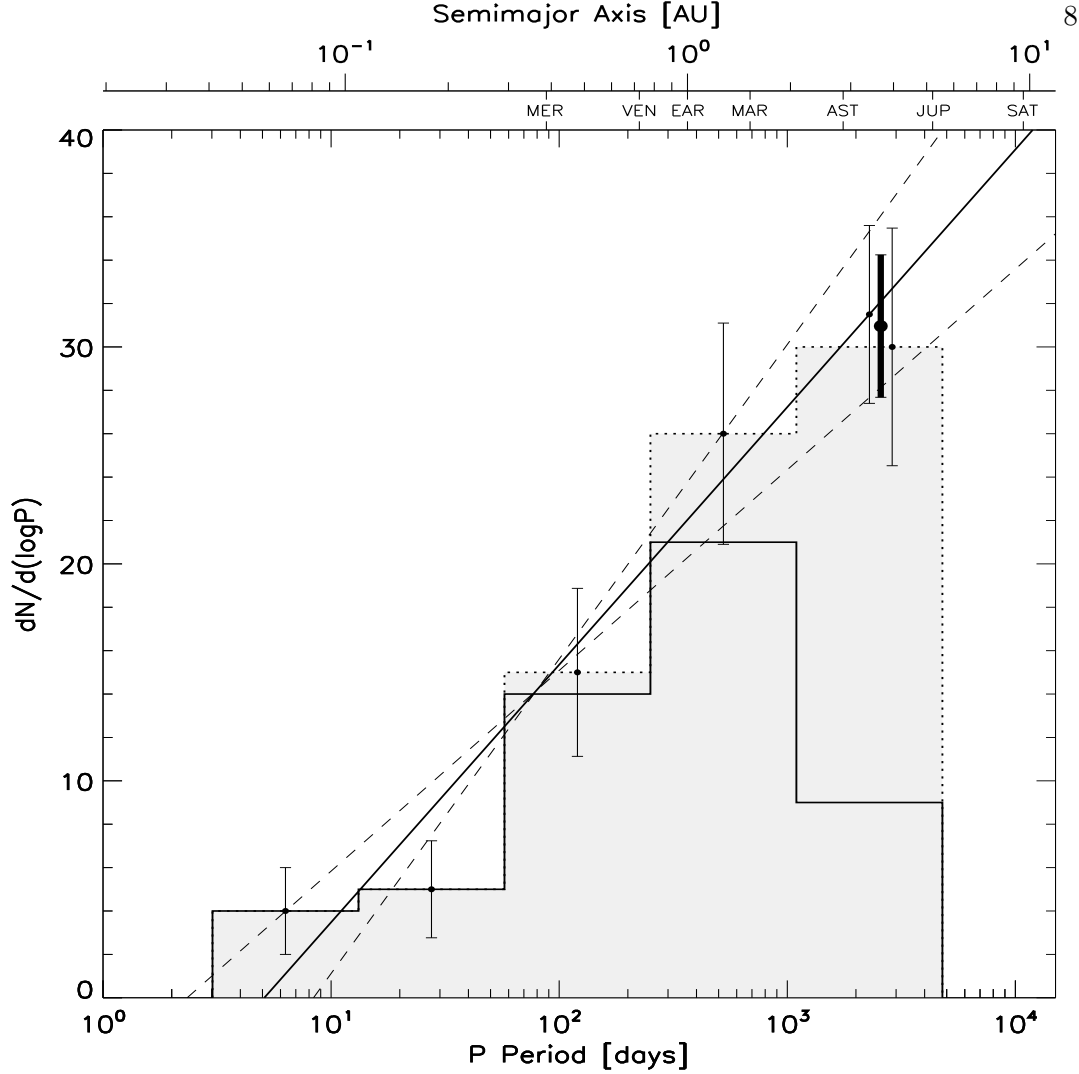
Fig. 4.— Trend in period of the corrected (dotted) and uncorrected (solid) less-biased subsample. The line is the best fit to the corrected histogram. The functional form fitted is linear in $logP$, i.e., $dN/d(logP) = a \, logP + b$. The best fit slope is $a = 12 \pm 3$. We estimate the number in the longest period bin ($1000 < P < 5000$ days) in two independent ways: 1) based on the extrapolation of the linear fit to this longer period bin and 2) correcting for undersampling in the "Being Detected" region as described in Section 2.2. The former yields 32 ± 4 while the later yields 30 ± 6. We take the weighted mean of these, 31 ± 3, as our best prediction for how many planets will be found in this longest period bin scattered over the mass range $0.84 < M \sin(i)/M_{\rm Jup} < 13$. To date, 9 extrasolar planets have been found in this period bin. Thus we predict that 22 ± 3 more planets will be found in this period bin.

Eight new planets were detected while this paper was in preparation (Vogt *et al.* 2002, Tinney *et al.* 2002). These are distinguished in Fig. 1 by crosses plotted over the dots. Five of the eight justify our parameter space partitions by falling as expected,

in the "Being Detected" region. The other three fall unexpectedly in the "Detected" region. If this region were fully detected newly detected planets would not fall there. However, two of the three (HD 68988 & HD 4203, both with $M \sin(i)$ between 1.5 and 2 $M_{\rm Jup}$) had only been observed for 1.5 years and therefore do not qualify for our least biased sample containing only host stars that have been monitored for at least three years. Therefore, these two apparent anomalies do not undermine our parameter space partitions. The third host lying in the "Detected" region lies near the "Being Detected" boundary. It has a two year period and was monitored for four years at the Anglo-Australian Telescope (AAT) (Tinney *et al.* 2002). Its observed velocity of ~ 50 m/s made it a $\sim 15\sigma$ signal with the AAT's ~ 3 m/s sensitivity. Its appearance in the "Detected" region may be ascribable to late reporting or may reflect the need to combine the constraints from Eqs. 1 & 2 into a smooth curve rather than two straight boundaries. Subsequent exoplanets can be similarly used to verify the accuracy of our representation of the Doppler detection selection effects in the $P - M \sin(i)$ plane.

2.3. Mass and Period Histogram Fits

The distribution of the masses of the exoplanets is shown against $M \sin(i)$ in Fig. 2 and against log $M \sin(i)$ in Fig. 3. The 6 planet correction (Section 2.2) to the $M \sin(i) \sim 1$ bin in both figures is indicated by the dotted lines. In Fig. 2 the solid curve and the enclosing dashed curves are the best fit and 68% confidence levels of the functional form $(dN/dM \sin i) \propto (M \sin i)^{\alpha}$ fit to the histogram of the corrected less-biased subsample ($50 = 44 + 6$ exoplanets). We find $\alpha = -1.5 \pm 0.2$. This means, for example, that within the same period range there are ~ 3 times as many $M_{\rm Jup}$ as 2 $M_{\rm Jup}$ exoplanets and similarly ~ 3 times as many 0.5 $M_{\rm Jup}$ as $M_{\rm Jup}$ exoplanets. This slope is steeper than the $\alpha \approx -1.0$ of previous analyses (Section 3.2).

In Fig. 3 the line is the best fit of the functional form $dN/d(log(M \sin i)) = a \ log(M \sin i) + b$ to the histogram. The best-fit slope, $a = -24 \pm 4$, is significantly steeper than flat. The extrapolation of this trend into the adjacent lower mass bin ($0.34 < M \sin(i)/M_{\rm Jup} < 0.84$) indicates that at least $\sim 36 \pm 3$ exoplanets with periods in the range $3 - 1000$ days are being hosted by the target stars now being monitored. Since 13 have been detected to date in this mass range, we predict that 23 ± 3 more have yet to be detected. Thus we predict that the continued monitoring of the target stars that produced the current set of exoplanets will eventually yield ~ 23 new planets in the parameter range $3 < P < 1000$ days with $0.34 < M \sin(i)/M_{\rm Jup} < 0.84$ (dotted horizontal rectangle in Fig. 1).

The trend of increasing number of exoplanets per box as one descends in mass does not hold true in the highly undersampled longest period bin ($1000 < P < 5000$). The absence of this trend may be the result of small number statistics or an additional

hint that a smooth curve, rather than our two straight boundaries, more accurately describes the selection effects.

Extrapolation of the linear trend found in Fig. 4 indicates that 22 new planets will be discovered in the first bin to the right of the rectangle in Fig. 1 ($1000 < P < 5000$ days in the mass range $0.84 < M\sin(i)/M_{\rm Jup} < 13$). Following the trend in $M\sin(i)$ identified in Fig. 3, these 22 should be preferencially assigned to the lower masses in this range. Extrapolation of the trend in period into an even longer period bin, which would include Saturn, is more problematic.

3. Discussion

3.1. Eccentricity

A significant difference between the detected exoplanets and Jupiter, is the high orbital eccentricities of the exoplanets. The eccentricities of the planets of our Solar System were presumably constrained to small values ($e \lesssim 0.1$) by the migration through, and accretion of, essentially zero eccentricity disk material. A simple model that can explain the higher exoplanet eccentricities is that in higher metallicity systems, the higher abundance of refractory material in the protoplanetary disk may lead to the production of more planetary cores in the ice zone producing multiple Jupiters which gravitationally scatter off each other. Occasionnaly one will be scattered in closer to the central star and become Doppler-detectable (Weidenschilling & Marzari 1996). If that is the origin of the hot jupiters, then the detected exoplanets may be the high metallicity tail of a distribution in which our Solar System is typical, and as longer period giant planets are found they will have lower eccentricities, comparable to Jupiter's and Saturn's. Thus, if Jupiter is the norm rather than the exception, not only will we find more planets in the $P - M\sin(i)$ parameter space near Jupiter as reported above, but also the eccentricities of the longer period exoplanets will be lower. The general distribution of the eccentricities of the exoplanets does not seem to reflect this, but exoplanets in planetary systems lend some support to the idea (see Fig. 5 and caption).
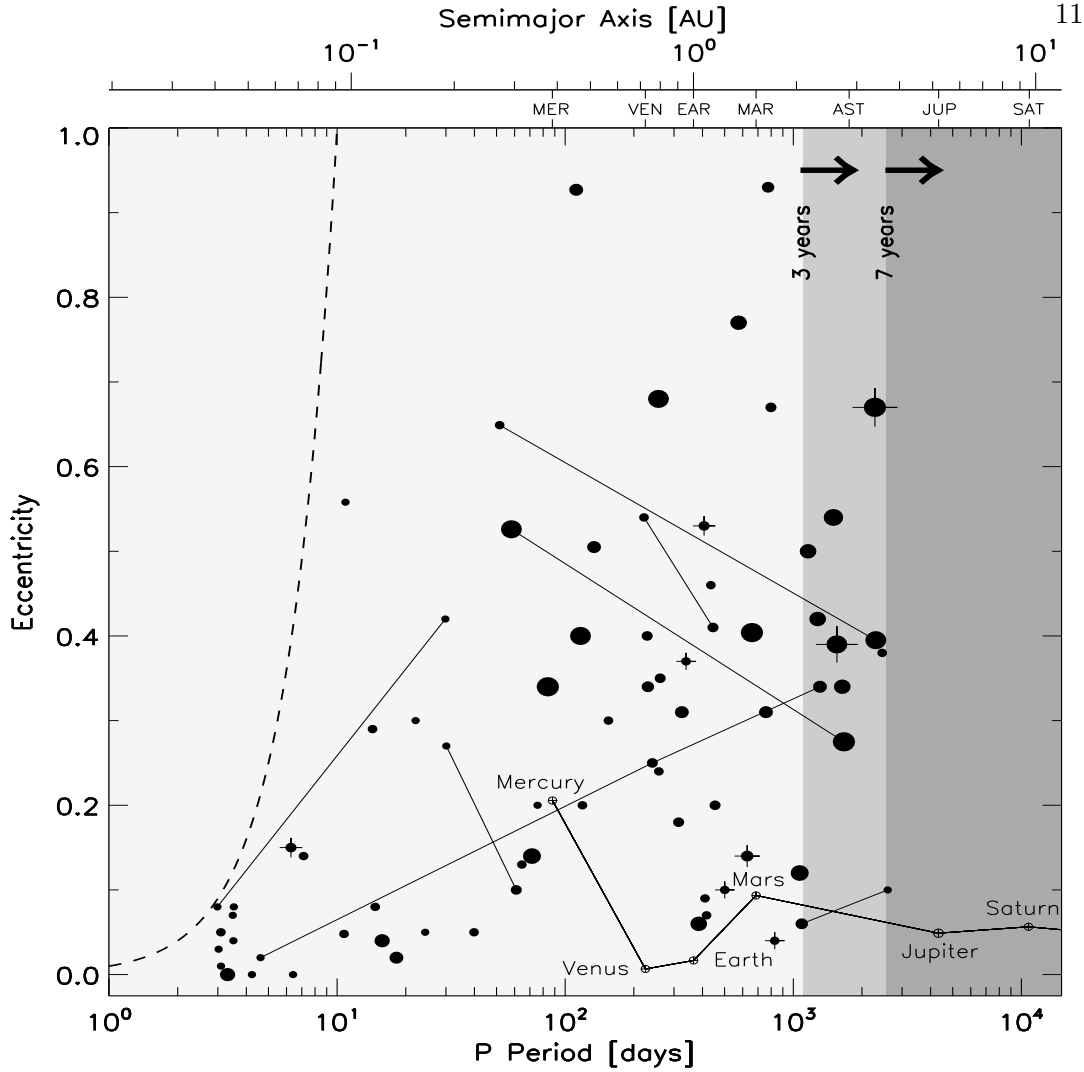
Fig. 5.— Eccentricity of the orbits of exoplanets as a function of period. Planets in the same system are connected by lines. Notice that in four out of the seven planetary systems the more distant member is less eccentric and more massive. This is what one would expect if the Solar System is a typical planetary system and Doppler-detectable exoplanets have been scattered in by more massive, less eccentric companions. This also suggests that the exoplanets closer to Jupiter's region of $P - M \sin(i)$ parameter space may share Jupiter's low eccentricity. In two of the planetary systems that do not conform to this pattern, the inner planet is so close to the central star that its orbit has probably been tidally circularized – an r^{-3} effect indicated by the dashed line. In the one remaining exception, the eccentricities are low and do resemble the planets of our Solar System. Thus, in planetary systems, the eccentricities of exoplanets with longer periods (like Jupiter's) tend to also have less eccentric orbits (like Jupiter's). Both the high metallicity of exoplanet hosts and this trend in eccentricity lend some support to the gravitational scattering model for the origin of hot jupiters, suggesting that Jupiter is a fairly typical massive planet of the more typical lower metallicity systems. As more exoplanetary systems are detected this pattern can be readily tested. Pointsize is proportional to exoplanet mass.

3.2. Fitting for α

In this paper we have focused on the position of Jupiter relative to the exoplanets. This relative comparison does not require a conversion of exoplanet $M\sin(i)$ values to M values (Jorissen *et al.* 2001, Zucker & Mazeh 2001a, 2001b and Tabachnik & Tremaine 2001). However, for this comparison Jupiter's position needs to be lowered and spread out a bit. Given a random distribution of orbital inclinations, the probability of $y = M\sin(i)$, given M, is

$$P(y|M) = \frac{y}{M^2\sqrt{1 - \frac{y^2}{M^2}}}. \tag{3}$$

With $M = M_{\mathrm{Jup}}$, this probability is the curve placed outside the plotting area on the lower right of Fig. 1. It represents the region of $M\sin(i)$ that Jupiter-mass planets would fall in when observed at random orientations. The mean of this distribution is $\pi/4 \approx 0.79$ while the median is 0.87 (in units of M_{Jup}). This lowers and spreads out in $M\sin(i)$ the position of Jupiter but does not change the main results of the extrapolations done here.

The functional form $dN/d(M\sin i) \propto (M\sin i)^{\alpha}$ can be fit in various ways to various versions of the $M\sin(i)$ histogram of exoplanets. When the histogram of all 74 exoplanets is fit, including the highly undersampled lowest $M\sin(i)$ bin, the result is $\alpha = -0.8$. This is reported in Marcy *et al.* 2001 and we confirm this result. This value for α is close to the $\approx -0.8 \pm 0.2$ found for very low mass stars (Bejar *et al.* 2001). When the lowest exoplanet $M\sin(i)$ bin is ignored because of known incompleteness we obtain $\alpha = -1.1$. This is very similar to the $\alpha \approx -1.1$ found in fits to the derived M distribution (Zucker & Mazeh 2001a, Tabachnik & Tremaine 2001). The fit for α seems to be more dependent on how the first bin is treated and how the sample for fitting is selected than on whether one fits to $M\sin(i)$ or M.

Fitting to the $M\sin(i)$ histogram of the less biased sample of 44 exoplanets, uncorrected for undersampling, yields $\alpha = -1.3$. After correcting for undersampling as described in Section 2.2 we obtain our final result: $\alpha = -1.5 \pm 0.2$ (Fig. 2). This slope is steeper than the $\alpha \approx -1.0$ of previous analyses and indicates that instead of M_{Jup} mass exoplanets being twice as common as $2\,M_{\mathrm{Jup}}$ exoplanets, they are three times as common.

4. Summary

Despite the fact that massive planets are easier to detect, the mass distribution of detected planets is strongly peaked toward the lowest detectable masses. And despite the fact that short period planets are easier to detect, the period distribution

is strongly peaked toward the longest detectable periods. To quantify these trends as accurately as possible, we have identified a less-biased subsample of exoplanets (Fig. 1). Within this subsample, we have identified trends in $M \sin(i)$ and period that are less biased than trends based on the full sample of exoplanets. Straightforward extrapolations of the trends quantified here, into the area of parameter space occupied by Jupiter, indicates that Jupiter lies in a region of parameter space densely occupied by exoplanets.

Our analysis indicates that 45 new planets will be detected in the parameter space discussed in the text. This estimate of 45 is a lower limit in the sense that if a smooth curve, rather than our two straight boundaries, more accurately describes the selection effects in Fig 1, larger corrections to the bin numbers would steepen the slopes in both Fig. 3 & 4.

Despite the importance of the mass distribution and the trends in it, it is the trend in period that, when extrapolated, takes us to Jupiter and the parameter space occupied by Jupiter-like exoplanets (compare Figs. 1 & 4). Long term slopes in the velocity data that have not yet been associated with planets are present in a large fraction of the target stars surveyed with the Doppler technique (Butler, Mayor private communication). However, quantifying the percentage of host stars showing such residual trends is difficult and depends on instrumental noise, phase coverage and the signal to noise threshold used to decide whether there is, or is not, a long term trend.

Figure 6 shows that the Doppler technique has been able to sample a very specific high mass, short-period region of the $logP - logM \sin(i)$ plane. Thus far, this sampled region does not overlap with the 10 times larger area of this plane occupied by the nine planets of our Solar System. Thus there is room in the $\sim 95\%$ of target stars with no Doppler-detected planets, to harbour planetary systems like our Solar System.

The trends in the exoplanets detected thus far do not rule out the hypothesis that our Solar System is typical. They support it. The extrapolations of the trends quantified here put Jupiter in the most densely occupied region of the $P - M \sin(i)$ parameter space. Our analysis suggests that Jupiter is more typical than indicated by previous analyses – instead of M_{Jup} mass exoplanets being twice as common as $2\,M_{\mathrm{Jup}}$ planets we find they are three times as common. In addition long term trends in velocity, not yet identified with planets, are common. Both of these observations indicate that the detected exoplanets are the observable tail of the main concentration of massive planets of which Jupiter is likely to be a typical member rather than an outlier.

Null results from microlensing searches have been used to constrain the frequency of Jupiter-mass planets (Gaudi et al. 2002). These are plotted in Fig. 6. Less than 33% of the lensing objects (presumed to be Galactic bulge M-dwarfs) have planetary companions within the dashed wedge-shaped area (the period scale, but not the AU

scale, is applicable to this area). A conversion of the relative frequencies reported here to a fractional abundance in the wedge-shaped area yields the rough estimate that more than ~ 3 percent of Doppler-surveyed Sun-like stars will be found to have companions with masses and periods in the wedge-shaped area. Thus our results are crudely consistent with current microlensing constraints. However, because of the difference in host mass, ($\sim M_{Sun}$ for Doppler surveys and $\sim 0.3 M_{Sun}$ for microlensing) it is not clear that such a direct comparison is meaningful. For example, if in the next few years Doppler and microlensing constraints appear to conflict, it may simply be that typical planetary masses scale with the mass of the host star, that is, Jupiter-mass planets at Jupiter-like orbital radii may be more common around $\sim M_{Sun}$ stars than around $\sim 0.3 M_{Sun}$ stars.
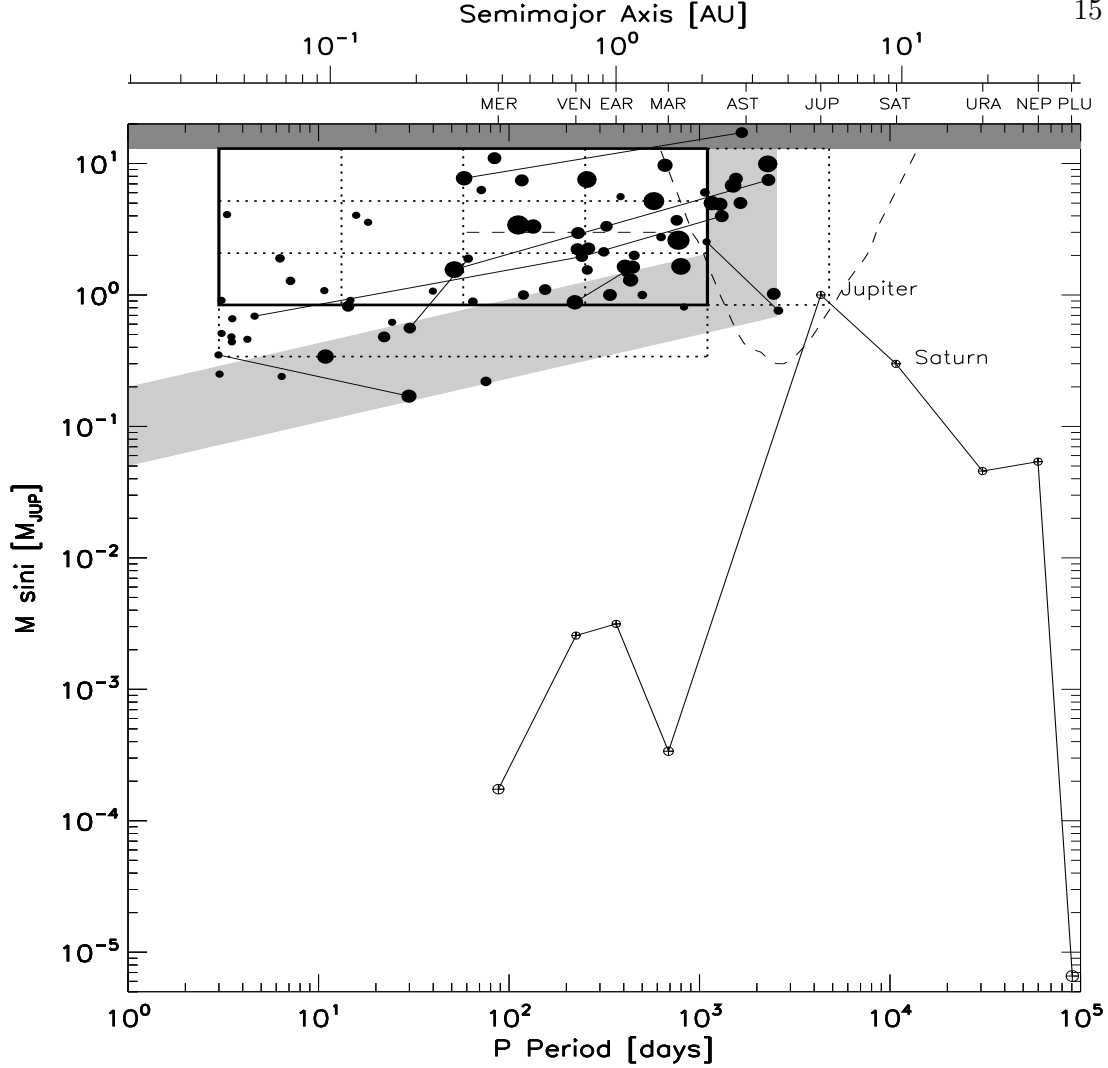
5. Acknowledgements

Fig. 6.— The region of the $P - M\sin(i)$ plane occupied by our Solar System compared to the region being sampled by Doppler surveys. Doppler surveys are on the verge of detecting Jupiter-like exoplanets. The lines, symbols and shading are the same as in Fig. 1. We would like to know how planetary systems in general are distributed in this plane. Extrapolations of the trends quantified in this paper put Jupiter in the most densely occupied region of the $P - M\sin(i)$ parameter space indicating that the detected exoplanets are the observable tail of the main concentration of massive planets that occupies the parameter space closer to Jupiter. If our Solar System is typical then the dispersion away from Jupiter into the Doppler-detectable region of this plot may be largely due to the effect of high metallicity in producing gravitational scattering. Whether Jupiter is slightly more or less massive than the average most massive planet in a planetary system is difficult to determine. However, the strong correlation between the presence of Doppler-detectable exoplanets and high host metallicity (e.g. Lineweaver 2001) suggests that high metallicity systems preferentially produce massive Doppler-detectable exoplanets. This further suggests (since the Sun is more metal-rich than $\sim 2/3$ of local solar analogues) that Jupiter may be slightly more massive than the average most massive planet of an average metallicity, but otherwise Sun-like, star. The dashed wedge-shaped contour represents the microlensing constraints discussed in the text.

6.   References

Beckwith, S.V.W., Henning, T. & Nakagawa, Y 2000, "Dust Properties and Assembly of Large Particles in Protoplanetary Disks" In "Protostars and Planets IV" edt V. Mannings, A.P. Boss & S.S. Russell, pp 533-558, Univ. Arizona Press, Tucson

Bejar, V.J.S. *et al.* 2001 'The Substellar Mass Function of Sigma Orionis' ApJ, 556, 830-836

Boss, A.P. 1995 "Proximity of Jupiter-like Planets to Low-mass Stars" Science, 267, 360

Gaudi, B.S. *et al.* 2002, "Microlensing Constraints on the Frequency of Jupiter-Mass Companions: Analysis of Five Years of PLANET Photometry", ApJ, 566, 463

Habing, H.J. *et al.* 1999, "Disappearance of stellar debris disks around main sequence stars after 400 million years" Nature, 401, 456-458

Haisch, K.E. *et al.* 2001, 'Disk Frequencies and Lifetimes of Young Clusters' ApJ, 553, L153-156

Henney, W.J. & O'Dell, C.R. 1999, 'A Keck High-Resolution Spectroscopic Study of the Orion Nebula Proplyds', AJ, 118, 2350-2368

Jorissen, A., Mayor, M. & Udry, S. 2001 "The distribution of exoplanet masses" A&A submitted, astro-ph/0105301

Kortenkamp & Wetherill, G.W. 2000,'Terrestrial Planet and Asteroid Formation in the Presence of Giant Planets' Icarus, 143, 60

Lineweaver, C.H. 2001, "An Estimate of the Age Distribution of Terrestrial Planets in the Universe: Quantifying Metallicity as a Selection Effect" Icarus, 151, 307-313

Lissauer, J.J. 1995, "Urey Prize Lecture: On the Diversity of Plausible Planetary Systems" Icarus, 114, 217-236

Marcy, G.W. *et al.*   2001 http://exoplanets.org/index.html and http://exoplanets.org/science.html

Marcy, G.W. & Butler, R.P. '2000 Millenium Essay: Planets Orbiting Other Suns' PASP 112, 137-140

Mayor, M. *et al.* 2001 Geneva Observatory http://obswww.unige.ch~udry/planet

Naef, D. *et al.* 2001, "The CORALIE survey for southern extrasolar planets V. 3 new extrasolar planets" astro-ph/0196255

Papaloizou, J.C.B. & Terquem, C. 1999, "Critical protoplanetary core masses in protoplanetary disks and the formation of short period giant planets" ApJ, 521, 823-828

Tabachnik, S. & Tremaine, S. 2001, "Maximum-likelihood method for estimating the mass and period distribution of extrasolar planets" astro-ph/0107482

Tinney, C.G. *et al.* , 2002 "Two Extra-solar Planets from the Anglo-Australian Planet Search" ApJ, submitted, astro-ph/0111255

Vogt, S. *et al.* 2002 "Ten Low Mass Companions from the Keck Precision Velocity Survey" ApJ, submitted, astro-ph/0110378

Ward, W. 1997 "Survival of Planetary Systems" ApJ, 482, L211-L214

Weidenschilling, S.J. & Marzari, F. 1996, "Gravitational Scattering as a possible origin for giant planets at small stellar distances" Nature, 384, 619-621

Wetherill, G.W. 1994, "Possible Consequence of absence of Jupiters in planetary systems" Ap&SS, 212, 23

Wetherill, G.W. 1995, "Planetary Science – how Special is Jupiter?" Nature, 373, 470

Zucker, S. & Mazeh, T. 2001a, "Derivation of the mass distribution of extrasolar Planets with MAXLIMA - a maximum likelihood Algorithm" astro-ph/0106042

Zucker, S. & Mazeh, T. 2001b, "Analysis of the Hipparcos Observations of Extrasolar Planets and the Brown Dwarf Candidates" astro-ph/0107142

Zuckerman, B., Forveille, T. & Kastner, J.H. 1995, 'Inhibition of giant-planet formation by rapid gas depletion around young stars?' Nature, 373, 494-496